Syntheses and Structures of New Luminescent Cyclometalated Palladium(II) and Platinum(II) Complexes: M(Bab)Cl, M(Br−Bab)Cl (M = Pd(II), Pt(II)), and $Pd_3Cl_4(Tab)_2$ (Bab = 1,3-bis(7-azaindolyl)phenyl, Br−Bab = 1-Bromo-3,5-bis(7-azaindolyl)phenyl, Tab =1,3,5-tris(7-azaindolyl)phenyl)

Datong Song, Qingguo Wu, Andrea Hook, Igor Kozin, and Suning Wang*

Department of Chemistry, Queen's University, Kingston, Ontario, K7L 3N6, Canada

Received March 26, 2001

The reactions of blue luminescent ligands 1,3-bis(7-azaindolyl)benzene (BabH), 1-bromo-3,5-bis(7-azaindolyl)benzene (Br−BabH), and 1,3,5-tris(7-azaindolyl)benzene (TabH) with K_2PdCl_4 and K_2PtCl_4 have been investigated. Five new luminescent cyclometalated palladium(II) and platinum(II) complexes Pd(Bab)Cl (**1**), Pt(Bab)Cl (**2**), Pd(Br−Bab)Cl (**3**), Pt(Br−Bab)Cl (**4**), and $Pd_3Cl_4(Tab)_2$ (**5**) have been synthesized and fully characterized. The molecular structures of **1** and **2**, and **3** and **4**, are similar. There are however significant variations in the solid-state structures and luminescence of **1** and **2**, and **3** and **4**. EHMO calculations revealed that it is most likely that the electronic transitions in the Pt(II) complexes are π to π^* transitions with significant contributions from d_π lone pairs of the Pt(II) center in the π level, and the electronic transitions in the Pd(II) complexes are either $d(z^2)$ to π^* charge-transfer transitions or π to π^* transitions similar to the Pt(II) complexes.

Introduction

Luminescent platinum(II) complexes have attracted much attention recently because of their potential applications in sensors and photochemical and electroluminescent devices.[1,2] In a recent report we described a group of novel blue luminescent organic molecules containing the 7-azaindolyl chromophore and their use as emitters in electroluminescent devices.[3] This new group of organic molecules shown in Chart 1 are bright blue emitters and have the potential to function as chelate ligands to transition metal ions because of the presence of nitrogen donor atoms and the possible chelation to metal centers by cyclometalation. Recent reports[2] by Thompson, Forrest, and co-workers on the successful use of red luminescent platinum(II) porphyrin complexes in electroluminescent devices have prompted us to investigate the potential of our new organic molecules as ligands in the formation of new luminescent Pt(II) complexes. For the purpose of comparison and understanding of the electronic properties of the ligand in the complex, we also investigated the reactions of the Pd(II) ion with the same group of ligands. Several new luminescent Pd(II) and Pt(II) complexes have been obtained and characterized (Chart 1). The details are presented herein.

(1) Paw, W.; Cummings, S. D.; Mansour, M. A.; Connick, W. B.; Geiger, D. K.; Eisenberg, R. *Coord. Chem. Rev.* **1998**, *171*, 125. (b) Cummings, S. D.; Eisenberg, R. *J. Am. Chem. Soc.* **1996**, *118*, 1949. (c) Huertas, S.; Hissler, M.; McGarrah, J. E.; Lachicotte, R. J.; Eisenberg, R. *Inorg. Chem.* **2001**, *40*, 1183. (d) Hissler, M.; Connick, W. B.; Geiger, D. K.; McGarrah, J. E.; Lipa, D.; Lachicotte, R. J.; Eisenberg, R. *Inorg. Chem.* **2000**, *39*, 447. (e) Wong, K. H.; Chan, M. C. W.; C. M. Che. *Chem. Eur. J.* **1999**, *5*, 2845. (f) Kunugi, Y.; Mann, K. R.; Miller, L. L.; Exstrom, C. L. *J. Am. Chem. Soc.* **1998**, *120*, 589. (g) Wong, W. Y.; Choi, K. H.; Cheah, K. W. *J. Chem. Soc., Dalton Trans.* **2000**, 113.

(2) Baldo, M. A.; O'Brien, D. F.; You, Y.; Shoustikov, A.; Sibley, S.; Thompson, M. E.; Forrest, S. R. *Nature* **1998**, *395*, 151. (b) O'Brien, D. F.; Baldo, M. A.; Thompson, M. E.; Forrest, S. R. *Appl. Phys. Lett.* **1999**, *74*, 442. (c) Kwong, R. C.; Sibley, S.; Dubovoy, T.; Baldo, M.; Forrest, S. R.; Thompson, M. E. *Chem. Mater.* **1999**, *11*, 3709. (d) Kwong, R. C.; Laman, S.; Thompson, M. E. *Adv. Mater.* **2000**, *12*, 1134.

(3) Wu, Q.; Lavigne, J. A.; Tao, Y.; D'Iorio, M.; Wang, S. *Chem. Mater.* **2001**, *13*, 71. (b) Wu, Q.; Hook, A.; Wang, S. *Angew. Chem., Int. Ed.* **2000**, *39*, 3933.

Experimental Section

All starting materials were purchased from Aldrich Chemical Co. All syntheses were carried out under a nitrogen atmosphere. Reagent-grade solvents were used without further purification. ^{1}H NMR spectra were recorded on Bruker Avance 300 or 400 MHz spectrometers. Excitation and emission spectra were recorded on a Photon Technologies International QuantaMaster Model 2 spectrometer. Emission lifetime was measured on a Photon Technolgies International Phosphorescent lifetime spectrometer, Timemaster C-631F equipped with a Xenon flash lamp, and digital emission photon multiplier tube using a band path of 5 nm for excitation and 2 nm for emission. Elemental analyses were performed by Canadian Microanalytical Service, Ltd, Delta, British Columbia. Melting points were determined on a Fisher-Johns melting point apparatus. The ligands listed in Figure 1 were synthesized according to the procedure described in a recent report.[3a]

Synthesis of [Pd(Bab)Cl] (1). BabH (0.50 mmol, 0.1505 g) and K_2PdCl_4 (0.50 mmol, 0.1632 g) were added to acetic acid (10 mL). The mixture was heated at 110−120 °C and refluxed for 6 h under N_2. After the reaction mixture was cooled to ambient temperature, the solid was collected by filtration and washed with 5 mL of acetic acid, CH_3OH, and diethyl ether,

10.1021/om010235z CCC: $20.00
Publication on Web 09/25/2001

Chart 1

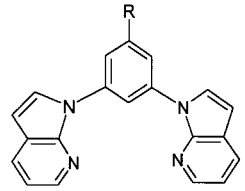

R = H, 1,3-bis(7-azaindoly)benzene, BabH

R = Br, 1-bromo-3,5-bis(7-azaindolyl)benzene, Br-BabH

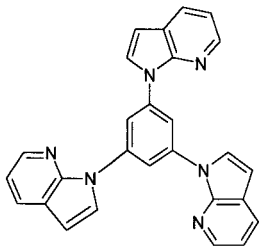

1,3,5-tris(7-azaindolyl)benzene, TabH

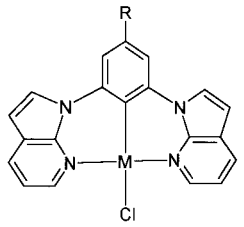

R = H, M = Pd, 1; M = Pt, 2
R = Br, M = Pd, 3; M = Pt, 4

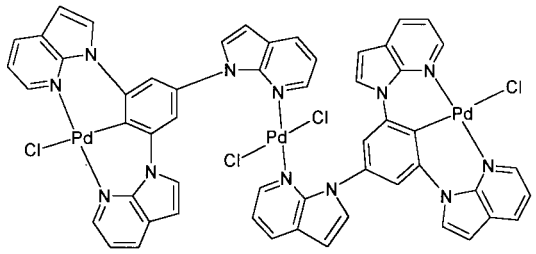

5

respectively. Recrystallization of the crude product from DMSO and methanol yielded light yellow crystals of **1** in a 89% yield. Mp >300 °C. ^{1}H NMR (DMSO-d_6, 25 °C): δ 9.02 (dd, $^3J_1 = 6.0$ Hz, $^3J_2 = 1.2$ Hz, 2H; 7-azain), 8.53 (dd, $^3J_1 = 7.8$ Hz, $^3J_2 = 1.2$ Hz, 2H; 7-azain), 8.36 (d, $^3J = 3.9$, 2H; 7-azain), 7.45−7.38 (m, 3H; benzene), 7.33 (dd, $^3J_1 = 7.5$ Hz, $^3J_2 = 6.0$ Hz, 2H; 7-azain), 7.03 (d, $^3J = 3.6$ Hz, 2H; 7-azain). Anal. Calcd for $C_{20}H_{13}N_4ClPd\cdot0.5H_2O$: C 52.19, H 3.07, N 12.17. Found: C 51.97, H 3.03, N 11.78.

Synthesis of [Pt(Bab)Cl] (2). To a solution of K_2PtCl_4 (0.20 mmol, 0.083 g) in a minimal amount of water was added a solution of BabH (0.20 mmol, 0.062 g) in 20 mL of CH_3CN. The mixture was stirred and refluxed for 6 h under N_2. After the reaction mixture was cooled to ambient temperature, the solid was collected by filtration and washed with 5 mL of water, CH_3OH, and diethyl ether, respectively. Recrystallization of the crude product from CH_2Cl_2 and hexanes yielded colorless crystals of **2** in a 53% yield. Mp >300 °C. ^{1}H NMR (CD_2Cl_2, 25 °C): δ 9.41 (dd, satellite, $^3J_1 = 6.0$ Hz, $^3J_2 = 1.2$ Hz, $^3J_{Pt-H} = 45$ Hz, 2H; 7-azain), 8.20 (dd, $^3J_1 = 7.8$ Hz, $^3J_2 = 1.2$ Hz, 2H; 7-azain), 8.05 (d, $^3J = 3.9$, 2H; 7-azain), 7.33 (dd, $^3J_1 = 8.7$ Hz, $^3J_2 = 6.9$ Hz, 1H; benzene), 7.17−7.24 (m, 4H; 7-azain and benzene), 6.91 (d, $^3J = 3.6$ Hz, 2H; 7-azain). Anal. Calcd for $C_{20}H_{13}N_4ClPt\cdot1.5CH_2Cl_2$: C 38.68, H 2.40, N 8.40. Found: C 38.69, H 2.65, N 8.43.

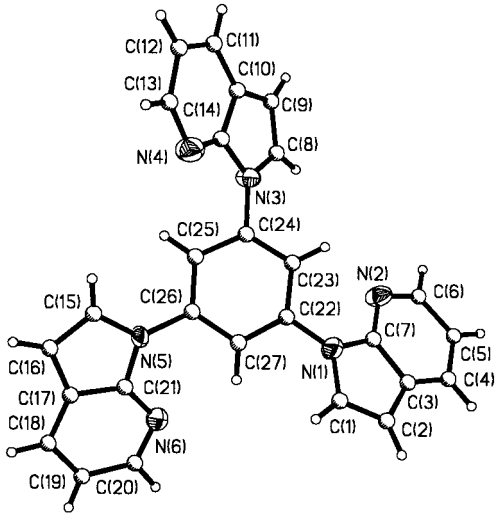

Figure 1. Diagram showing the molecular structure of TabH with labeling schemes and 50% thermal ellipsoids.

Synthesis of [Pd(Br−Bab)Cl] (3). Br−BabH (0.50 mmol, 0.1946 g) and K_2PdCl_4 (0.50 mmol, 0.1632 g) were added to acetic acid (10 mL). The mixture was heated at 110−120 °C and refluxed for 6 h under N_2. After the reaction mixture was cooled to ambient temperature, the solid was collected by filtration and washed with 5 mL of acetic acid, CH_3OH, and diethyl ether, respectively. Recrystallization of the crude product from DMSO and methanol yielded light yellow crystals of **3** in a 91% yield. Mp >300 °C. ^{1}H NMR (DMSO-d_6, 25 °C): δ 9.20 (dd, $^3J_1 = 6.0$ Hz, $^3J_2 = 1.2$ Hz, 2H; 7-azain), 8.60 (d, $^3J = 3.9$ Hz, 2H; 7-azain), 8.38 (dd, $^3J_1 = 7.5$ Hz, $^3J_2 = 1.2$ Hz, 2H; 7-azain), 7.65 (s, 2H; benzene), 7.36 (dd, $^3J_1 = 7.5$ Hz, $^3J_2 = 6.0$ Hz, 2H; 7-azain), 7.05 (d, $^3J = 3.6$ Hz, 2H; 7-azain). Anal. Calcd for $C_{20}H_{12}N_4ClBrPd\cdot0.5H_2O$: C 45.32, H 2.28, N 10.57. Found: C 45.15, H 2.35, N 10.57.

Synthesis of [Pt(Br−Bab)Cl] (4). To a solution of K_2PtCl_4 (0.30 mmol, 0.125 g) in minimal amount of water was added a solution of Br−BabH (0.30 mmol, 0.1167 g) in 20 mL of CH_3CN. The mixture was stirred and refluxed for 12 h under N_2. After the reaction mixture was cooled to ambient temperature, the solid was collected by filtration and washed with 5 mL of water, CH_3OH, and diethyl ether, respectively. Recrystallization of the crude product from CH_2Cl_2 and hexanes yielded colorless needles of **4** in a 26% yield. Mp >300 °C. ^{1}H NMR ($CDCl_3$, 25 °C): δ 9.45 (dd, satellite, $^3J_1 = 6.0$ Hz, $^3J_2 = 1.2$ Hz, $^3J_{Pt-H} = 45$ Hz, 2H; 7-azain), 8.25 (dd, $^3J_1 = 7.5$ Hz, $^3J_2 = 1.2$ Hz, 2H; 7-azain), 7.90 (d, $^3J = 3.9$, 2H; 7-azain), 7.33 (s, 2H; benzene), 7.17 (dd, $^3J_1 = 7.5$ Hz, $^3J_2 = 6.0$ Hz,2H; 7-azain), 6.85 (d, $^3J = 3.6$ Hz, 2H; 7-azain). Anal. Calcd for $C_{20}H_{12}N_4ClBrPt$: C 38.80, H 1.94, N 9.05. Found: C 38.53, H 1.96, N 9.01.

The synthesis of $[Pd_3(Tab)_2Cl_4]$ (**5**) has been given in a previous report.[3b]

X-ray Crystallography Analysis. Single crystals of Br−BabH were obtained from CH_2Cl_2/hexane, and single crystals of TabH and **4** were grown from CH_3CN/ethanol and CH_2Cl_2/hexanes solutions, respectively. Single crystals of **1**−**3** and **5** suitable X-ray diffraction analysis were obtained from either a DMSO/ethanol or a DMF/ethanol solution. All crystals were

Table 1. Crystallographic Data

	Br−BabH	TabH	**1**	**2**	**3**	**4**	**5**
formula	$C_{20}H_{13}N_4Br$	$C_{27}H_{18}N_6$	$C_{20}H_{13}N_4ClPd$	$C_{20}H_{13}N_4ClPt$	$C_{20}H_{12}N_4BrClPd$	$C_{20}H_{12}N_4BrClPt$	$C_{54}H_{34}N_{12}Cl_4Pd_3 \cdot 2(CH_3)_2NCHO$
fw	389.25	426.47	451.9	539.88	530.84	618.78	1457.06
space group	$P2_1/c$	$Pna2_1$	$Cmca$	$C2/c$	$P2_1/c$	$P2_1/n$	$P2_1/c$
a, Å	7.038(1)	20.95(3)	13.2189(10)	15.579(2)	8.4665(6)	10.551(7)	9.1343(6)
b, Å	9.1710(16)	24.92(3)	9.2246(7)	13.826(2)	9.8198(8)	8.004(5)	15.6271(10)
c, Å	25.813(5)	3.848(5)	13.8922(11)	7.7807(11)	21.045(2)	40.69(2)	20.3907(15)
α, deg	90	90	90	90	90	90	90
β, deg	90.370(3)	90	90	101.37(2)	95.762(2)	96.303(9)	102.153(1)
γ, deg	90	90	90	90	90	90	90
V, Å^3	1666.2(5)	2010(5)	1694.0(2)	1644.4(4)	1740.8(2)	3416(4)	2845.4(3)
Z	4	4	4	4	4	8	2
D_{calc}, g cm^{-3}	1.552	1.410	1.769	2.181	2.023	2.407	1.702
T, °C	23	23	23	23	23	23	23
μ, cm^{-1}	24.77	0.87	12.64	87.07	35.28	107.26	11.84
2θ, max, deg	56.7	56.7	47	56.5	46.5	56.5	46.5
no. of reflns measd	11705	13024	3281	5966	7168	19121	11925
no. of reflns used	3943	3914	643	1975	2513	7505	4090
no. of params	274	299	116	146	244	428	376
final R ($I>2\sigma(I)$)	$R_1{}^a = 0.0438$	$R_1 = 0.0759$,	$R_1 = 0.0227$,	$R_1 = 0.0269$,	$R_1 = 0.0340$,	$R_1 = 0.1305$,	$R_1 = 0.0356$,
	$wR_2{}^b = 0.1025$	$wR_2 = 0.1274$	$wR_2 = 0.0659$	$wR_2 = 0.0485$	$wR_2 = 0.0709$	$wR_2 = 0.2909$	$wR_2 = 0.0719$
R (all data)	$R_1 = 0.0625$	$R_1 = 0.3013$,	$R_1 = 0.0256$,	$R_1 = 0.0322$,	$R_1 = 0.0560$,	$R_1 = 0.1979$,	$R_1 = 0.0621$,
	$wR_2 = 0.1068$	$wR_2 = 0.1658$	$wR_2 = 0.0690$	$wR_2 = 0.0492$	$wR_2 = 0.0758$	$wR_2 = 0.3127$	$wR_2 = 0.0779$
goodness of fit on F^2	0.947	0.798	1.166	0.969	0.857	1.107	0.881

[a] $R_1 = \sum||F_o| - |F_c||/\sum|F_o|$. [b] $wR_2 = [\sum w[(F_o^2 - F_c^2)^2]/\sum[w(F_o^2)^2]]^{1/2}$. [c] $w = 1/[\sigma^2(F_o^2) + (0.075P)^2]$, where $P = [\mathrm{Max}(F_o^2, 0) + 2F_c^2]/3$.

mounted on glass fibers. All data were collected on a Siemens single-crystal P4 X-ray diffractometer with a Bruker SMART CCD 1000 detector and monochromated Mo Kα radiation operating at 50 kV and 35 mA at 23 °C. The data collection 2θ ranges are 2−47° for **1**, **3**, and **5** and 3.50−57° for Br−BabH, TabH, **2**, and **4**, respectively. No significant decay was observed during the data collection. Data were processed on a Pentium PC using the Bruker AXs Window NT SHELXTL software package (Version 5.10).[4] Neutral atom scattering factors were taken from Cromer and Waber.[5] Empirical absorption correction was applied to all crystals. The crystals of Br−BabH and **2**−**5** belong to monoclinic space groups $P2_1/c$, $C2/c$, and $P2_1/n$, respectively, while the crystals of TabH and **1** belong to the othorhombic space groups $Pna2_1$ and $Cmca$, respectively. All structures were solved by direct methods. DMF solvent molecules were located in the lattice of **5** (2 DMF per molecule of **5**). There are two independent molecules in the asymmetric unit of **4**. Compound **1** is disordered over two sites related by a 2/m symmetry. The disorder of **1** was modeled successfully. The crystal of **4** has a very long c axis (40.69(2) Å), which is believed to be the cause of the poor data quality of **4**. All non-hydrogen atoms except those in the disordered molecule of **1** and some of the nitrogen and carbon atoms in **4** were refined anisotropically. The positions of hydrogen atoms were either determined directly from the difference Fourier maps or calculated, and their contributions in structural factor calculations were included. The crystal data are summarized in Table 1. Selected bond lengths and angles for **1**−**5** are given in Table 2.

(4) *SHELXTL* NT crystal structure analysis package; Bruker Axs, Analytical X-ray System: Madison, WI, 1999; Version 5.10.

(5) Cromer, D. T.; Waber, J. T. *International Tables for X-ray Crystallography*; Kynoch Press: Birmingham, AL, 1974; Vol. 4, Table 2.2A.

Results and Discussion

Syntheses and Structures. Ligands. The ligands 1,3-bis(7-azaindolyl)benzene (BabH), 1-bromo-3,5-bis(7-azaindolyl)benzene (Br−BabH), and 1,3,5-tris(7-azaindolyl)benzene (TabH) were synthesized by using Ullmann condensation reactions[6] between 7-azaindole and the appropriate brominated benzene using procedures described in a previous report.[3a] The crystal structure of BabH reported previously revealed a chiral arrangement of BabH molecules in the crystal lattice (space group $P2_12_12_1$). Luminescent chiral crystals have some unique properties and applications, one of which is their potential to display triboluminescence,[7] which prompted us to investigate the crystal structures of Br−BabH and TabH in order to confirm if these two molecules also have a chiral arrangement in the crystal lattice. Br−BabH forms block crystals. The molecular structure of Br−BabH is similar to that of BabH (the details are given in the Supporting Information). However, in contrast to BabH, Br−BabH crystallizes in the centric space group $P2_1/c$. The crystals of TabH are long thin needles and belong to the chiral space group $Pna2_1$. As shown in Figure 1, TabH has a nonplanar structure with an approximate C_3 rotation symmetry. The molecules of TabH stack along the c axis with an intermolecular

(6) Goodbrand, H. B.; Hu, N. X. *J. Org. Chem.* **1999**, *64*, 670. (b) Lindley, J. *Tetrahedron* **1984**, *40*, 1433. (c) Fanta, P. E. *Synthesis* **1974**, 1.

(7) Sweeting, L. M.; Rheingold, A. L.; Gingerich, J. M.; Rutter, A. W.; Spence, R. A.; Cox, C. D.; Kim, T. J. *Chem. Mater.* **1997**, *9*, 1103. (b) Clegg, W.; Sage, I.; Oswald, I.; Brough, P.; Bourhill, G. *Acta Crystallogr. C* **2000**, *56*, 1323. (c) Ronfard, H. J. C.; Valat, P.; Wintgens, V.; Kossanyi, J. *J. Lumin.* **2000**, *91*, 71.

Table 2. Selected Bond Lengths [Å] and Angles [deg]

1				**2**			
Pd(1)−C(8)	1.95(2)	C(8)−Pd(1)−N(1)	90.000(1)	Pt(1)−C(11)	2.014(5)	N(1a)−Pt(1)−N(1)	178.69(16)
Pd(1)−N(1)	2.031(4)	N(1a)−Pd(1)−N(1)	180.00(19)	Pt(1)−N(1)	2.014(3)	N(1)−Pt(1)−C(11)	90.65(8)
Pd(1)−Cl(1)	2.403(6)	C(8)−Pd(1)−Cl(1)	180.000(2)	Pt(1)−Cl(1)	2.3883(13)	N(1)−Pt(1)−Cl(1)	89.35(8)
N(1)−C(4)	1.324(7)	N(1)−Pd(1)−Cl(1)	90.000(1)	N(1)−C(7)	1.346(5)	C(11)−Pt(1)−Cl(1)	180.0
N(1)−C(5)	1.359(7)	C(4)−N(1)−Pd(1)	119.1(3)	N(1)−C(1)	1.364(5)	C(7)−N(1)−Pt(1)	120.2(3)
C(1)−N(2)	1.428(9)	C(5)−N(1)−Pd(1)	122.9(3)	N(2)−C(7)	1.371(5)	C(1)−N(1)−Pt(1)	124.1(3)
N(2)−C(4)	1.360(8)	C(9)−C(8)−Pd(1)	124.0(8)	N(2)−C(6)	1.400(5)	C(8)−C(11)−Pt(1)	121.6(2)
N(2)−C(9)	1.424(9)			N(2)−C(8)	1.421(5)		

3				**4**			
Pd(1)−C(16)	1.995(5)	C(16)−Pd(1)−N(1)	90.6(2)	Pt(1)−C(20)	1.98(3)	N(8)−C(33)	1.23(3)
Pd(1)−N(1)	2.031(5)	C(16)−Pd(1)−N(3)	90.0(2)	Pt(1)−N(3)	2.00(3)	N(8)−C(39)	1.40(3)
Pd(1)−N(3)	2.042(5)	N(1)−Pd(1)−N(3)	177.09(18)	Pt(1)−N(1)	2.03(2)		
Pd(1)−Cl(1)	2.3867(16)	C(16)−Pd(1)−Cl(1)	176.81(16)	Pt(1)−Cl(1)	2.377(9)	C(20)−Pt(1)−N(3)	91.9(11)
Br(1)−C(19)	1.899(6)	N(1)−Pd(1)−Cl(1)	90.89(14)	N(1)−C(7)	1.28(4)	C(20)−Pt(1)−N(1)	90.1(10)
N(1)−C(7)	1.332(6)	N(3)−Pd(1)−Cl(1)	88.60(14)	N(1)−C(1)	1.39(4)	N(3)−Pt(1)−N(1)	177.2(11)
N(1)−C(1)	1.357(7)	C(7)−N(1)−Pd(1)	120.0(4)	Br(1)−C(17)	1.91(4)	C(20)−Pt(1)−Cl(1)	177.7(8)
N(2)−C(7)	1.370(6)	C(1)−N(1)−Pd(1)	122.5(4)	Pt(2)−C(40)	1.98(3)	N(3)−Pt(1)−Cl(1)	87.1(8)
N(2)−C(17)	1.418(6)	C(14)−N(3)−Pd(1)	119.7(4)	Pt(2)−N(7)	2.00(3)	N(1)−Pt(1)−Cl(1)	91.0(7)
N(2)−C(6)	1.431(6)	C(8)−N(3)−Pd(1)	122.8(4)	Pt(2)−N(5)	2.04(3)	C(7)−N(1)−Pt(1)	123(2)
N(3)−C(14)	1.332(7)	C(17)−C(16)−Pd(1)	123.7(4)	Pt(2)−Cl(2)	2.375(8)	C(1)−N(1)−Pt(1)	122(2)
N(3)−C(8)	1.346(7)	C(15)−C(16)−Pd(1)	121.7(4)	N(2)−C(6)	1.30(4)	C(40)−Pt(2)−N(7)	91.0(14)
N(4)−C(13)	1.344(7)			N(2)−C(7)	1.39(4)	C(40)−Pt(2)−N(5)	90.8(14)
N(4)−C(14)	1.403(7)			N(2)−C(15)	1.49(3)	N(7)−Pt(2)−N(5)	178.1(12)
N(4)−C(15)	1.413(6)			Br(2)−C(37)	1.96(3)	C(40)−Pt(2)−Cl(2)	175.8(11)
				N(3)−C(8)	1.34(4)	N(7)−Pt(2)−Cl(2)	90.4(8)
				N(3)−C(14)	1.37(4)	N(5)−Pt(2)−Cl(2)	87.8(8)
				N(4)−C(13)	1.34(4)	C(8)−N(3)−Pt(1)	123(2)
				N(4)−C(14)	1.34(4)	C(14)−N(3)−Pt(1)	122(2)
				N(4)−C(19)	1.40(4)	C(27)−N(5)−Pt(2)	122(3)
				N(5)−C(27)	1.24(4)	C(21)−N(5)−Pt(2)	109(2)
				N(5)−C(21)	1.44(4)	C(34)−N(7)−Pt(2)	121(2)
				N(6)−C(27)	1.36(4)	C(28)−N(7)−Pt(2)	121(2)
				N(6)−C(35)	1.48(4)	C(15)−C(20)−Pt(1)	126(2)
				N(6)−C(26)	1.50(4)	C(19)−C(20)−Pt(1)	119(2)
				N(7)−C(34)	1.35(4)	C(35)−C(40)−Pt(2)	123(3)
				N(7)−C(28)	1.36(4)	C(39)−C(40)−Pt(2)	124(3)

separation distance of 3.848(5) Å. All three ligands are bright blue emitters in solution and the solid state. However, preliminary tests on the crystals of BabH and TabH did not reveal any triboluminescence. TabH molecules have been used successfully as a blue emitter in electroluminescent devices.[3a]

Complexes. BabH, Br−BabH, and TabH have either two or three nitrogen donor atoms that can be used to coordinate to a metal center. In addition, the removal of the proton on the carbon atom at the 2 position would allow these ligands to chelate to a metal center as tridentate chelate ligands. Pd(II) and Pt(II) metal ions are well known for their ability to undergo orthometalation by activating a C−H bond.[8,9] It is therefore not surprising that we have found that the BabH, Br−BabH, and TabH ligands indeed react readily with Pt(II) and Pd(II) metal ions. We examined the reactions of K_2PtCl_4 and K_2PdCl_4 with BabH, Br−BabH, and TabH. Five new Pd(II) and Pt(II) complexes with these ligands have been isolated and characterized. The Pd(II) complexes Pd(Bab)Cl (**1**), Pd(Br−Bab)Cl (**3**), and $Pd_3(Tab)_2Cl_4$ (**5**) were obtained by reacting K_2PdCl_4 with the corresponding ligand in refluxing acetic acid using a procedure similar to that reported recently by Cádenas et al.[8] The Pt(II) complexes Pt(Bab)Cl (**2**) and Pt(Br−Bab)Cl (**4**) were obtained under a much milder reaction condition than those used for Pd(II) complexes, i.e., reacting K_2PtCl_4 with the corresponding ligand in refluxing CH_3CN. Attempts to synthesize the Pt(II) analogue of compound **5** were unsuccessful. Compounds **1**−**5** have a very poor solubility in common organic solvents such as CH_2Cl_2 and THF but are soluble in DMSO or DMF.

Compounds **1** and **2** are analogues with similar compositions and molecular structures. However, they crystallize in two very different space groups, orthorhombic *Cmca* versus monoclinic *C*2/*c*. The formation of the Pd−C and Pt−C bond in **1** and **2** is a consequence of cyclometalation of the BabH, favored by the geometry of the ligand and the chelating effect, a common phenomenon in organopalladium and organoplatinum compounds. However, previously reported cyclometalated Pd(II) or Pt(II) complexes typically have five-membered chelate rings.[8,9] The six-membered chelate ring observed in **1** and **2** is quite uncommon for organopalladium(II) and organoplatinum(II) complexes. The Pd(1) atom in **1** is situated on the 2/*m* symmetry element, and half of the molecule of **1** is in the asymmetric unit and disordered over two sites related by the 2/*m* symmetry operation. Figure 2 shows the molecular structure of **1** without the symmetry-related disordered set. The complete drawing of **1** is provided in the

(8) Cárdenas, D. J.; Echavarren, A. M. *Organometallics* **1999**, *18*, 3337.

(9) Van Houten, K. A.; Heath, D. C.; Barringer, C. A.; Rheingold, A. L.; Pilato, R. S. *Inorg. Chem.* **1998**, *37*, 4647. (b) Neve, F.; Crispini, A.; Campagna, S. *Inorg. Chem.* **1997**, *36*, 6150. (c) Lai, S. W.; Cheung, T. C.; Chan, M. C. W.; Cheung, K. K.; Peng, S. M.; Che, C. M. *Inorg. Chem.* **2000**, *39*, 255. (d) Albrecht, M.; Lutz, M.; Spek, A. L.; van Koten, G. *Nature* **2000**, *406*, 970. (e) Nonoyama, M.; Nakajima, K. *Polyhedron* **1999**, *18*, 533. (f) Lai, S. W.; Chan, M. C. W.; Cheung, K. K.; Peng, S. M.; Che, C. M. *Organometallics* **1999**, *18*, 3991.

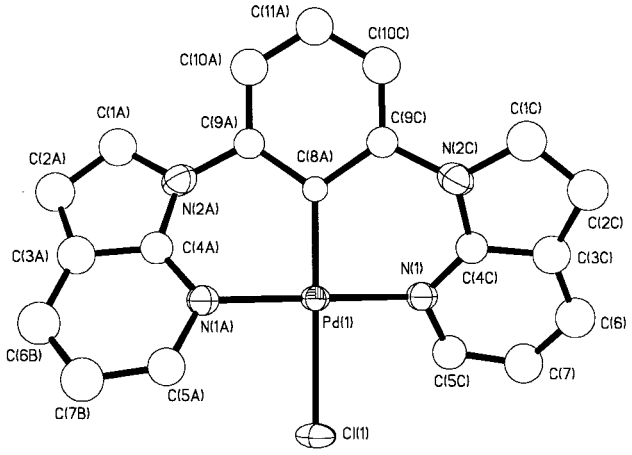

Figure 2. Diagram showing the molecular structure of **1** with disordered portion removed and labeling schemes and 50% thermal ellipsoids.

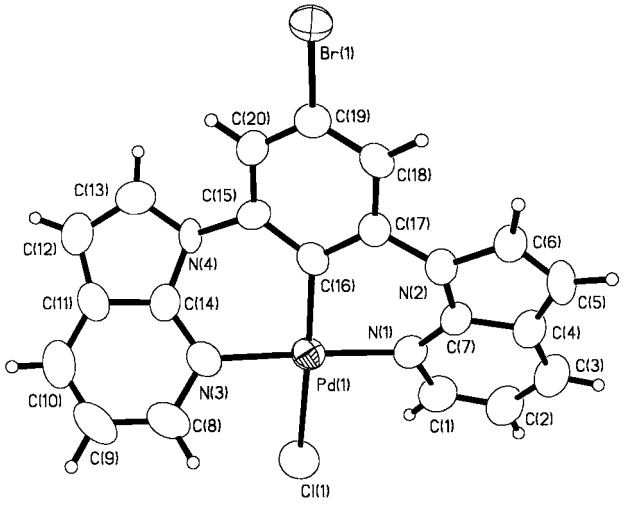

Figure 3. Diagram showing the molecular structure of **3** with labeling schemes and 50% thermal ellipsoids.

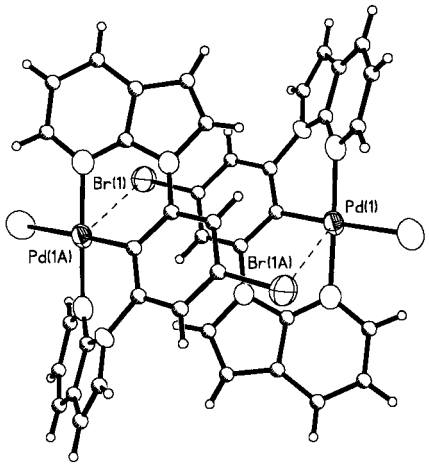

Figure 4. Diagram showing the dimer of **3** linked by weak Br···Pd interactions.

Supporting Information. The Bab ligand is chelated to the Pd(II) center in a nonplanar fashion with a dihedral angle of 78° between the Pd(1)−N(1)−C(4c) plane and the Pd(1)−N(1a)−C(4a) plane. The nonplanarity of **1** is obviously caused by the geometry of the ligand and the six-membered chelate ring. The Pd(1)−ligand bond distances in **1** are typical.[8,9] The shortest intermolecular Pd···Pd separation distance is 8.060(1) Å. The structure of **2** (provided in the Supporting Information) has a 2-fold rotation axis and is similar to that of **1** with typical Pt−N, Pt−C, and Pt−Cl bond lengths. The dihedral angle between the Pt(1)−N(1)−C(7) and Pt(1)−N(1a)−C(7a) planes is 72.9°, much smaller than that of **1**. The ^3J coupling constant of 45 Hz between the Pt atom and the hydrogen atom on C(1) was observed in the ^{1}H NMR spectrum of **2** and is consistent with previously reported $^3J_{Pt-H}$ coupling constants.[10] The most striking difference between **1** and **2** is that the molecules of **2** stack in the crystal lattice along the *c* axis with a Pt···Pt separation distance of 7.781(1) Å. In addition, the phenyl portion of the Bab ligand in **2** also stacks with a separation distance of 3.92 Å.

Compounds **3** and **4** are another pair of analogues but crystallize with two different unit cells. The $^3J_{Pt-H}$ coupling constant in **4** is identical to that of **2**. The molecular structure of **3** is shown in Figure 3 (the structure of **4** is provided in the Supporting Information). The bond lengths and angles of **3** and **4** are similar to those of **1** and **2**. The major difference between **3** and **4** is that the bromine atom on the phenyl ring in **3** has a weak interaction with the Pd(1) center in the neighboring molecule with a Pd(1)−Br(1a) distance of 4.037(1) Å, while no similar interaction is present in **4**. As a result of the weak Pd−Br interaction, molecules of **3** form pairs in the solid state with the phenyl rings stacking between the pair as shown in Figure 4. The shortest atomic separation distance between the stacked phenyl rings is 3.361 Å. The Pd(1)···Pd(1a) separation distance of 6.756(1) Å between the pair is the shortest Pd···Pd separation distance in the crystal lattice of **3**. As observed in **1** and **2**, compound **3** is not planar, with a dihedral angle of 70.4° between the Pd(1)−N(1)−C(7) and Pd(1)−N(3)−C(14) planes. The corresponding dihedral angle in **4** is much smaller, 62.4°. In contrast to **3**, the molecules of **4** stack along the *b* axis with a Pt···Pt separation distance of 5.477−5.480(1) Å. The Pt···Pt separation distances are too long for any possible metal−metal interactions. The observed difference of Pt−Pt and Pd···Pd separation distances in compounds **1**−**4** is believed to be responsible for the crystal lattice difference between **1** and **2** as well as **3** and **4**.

There are three Pd(II) ions in **5**. The Tab ligand acts as both a chelating ligand and a bridging ligand (Chart 1). Two of the 7-azaindolyl groups of the Tab ligand are chelated to the Pd(II) center in the same fashion as observed for Bab and Br−Bab ligands, while the third 7-azaindolyl group is coordinated to a second Pd(II) center as a terminal ligand, thus linking three Pd(II) ions together in a linear fashion. The separation distance between the neighboring Pd(II) ions in **5** is 5.866(1) Å, clearly imposed by the bridging Tab ligand. Details of the crystal structure of compound **5** can be found in a previous report.[3b]

Luminescent Properties. BabH, Br−BabH, and TabH are efficient blue emitters in solution and the solid state with emission maxima ranging from 392 to 428 nm. Their Pd(II) and Pt(II) complexes **1**−**5**, however, have no luminescence in solution at ambient tempera-

(10) Scott, J. D.; Puddephatt, R. J. *Organometallics* **1983**, *2*, 1643.

Table 3. Luminescent Data for Complexes 1−5 and the Corresponding Ligands

compound	excitation, λ_{max}, nm	UV absorption, nm	emission, λ_{max}, nm (τ, μs)	
1, Pd(Bab)Cl	383		554	solid, 77 K
		274, 302, 330	not emissive	CH_2Cl_2, 298 K
2, Pt(Bab)Cl	351		536	solid, 298 K
	321		464, 492 (242 ± 3)	CH_2Cl_2, 77 K
		260, 300	not emissive	CH_2Cl_2, 298 K
BabH	342	318	392	CH_2Cl_2, 298 K
	334		384	solid, 298 K
3, Pd(Br−Bab)Cl	370		573	solid, 77 K
		278, 314	not emissive	CH_2Cl_2, 298 K
4, Pt(Br−Bab)Cl	424		548 (16 ± 2)	solid, 298 K
	368		500 (414 ± 1)	solid, 77 K
		270, 325	not emissive	CH_2Cl_2, 298 K
Br−BabH	347	318	416	CH_2Cl_2, 298 K
	362		428	solid, 298 K
5, $Pd_3(Tab)_2Cl_4$	370		575	solid, 77 K
		280, 326	not emissive	CH_2Cl_2, 298 K
TabH	344	314	392	CH_2Cl_2, 298 K
	362		412	solid, 298 K

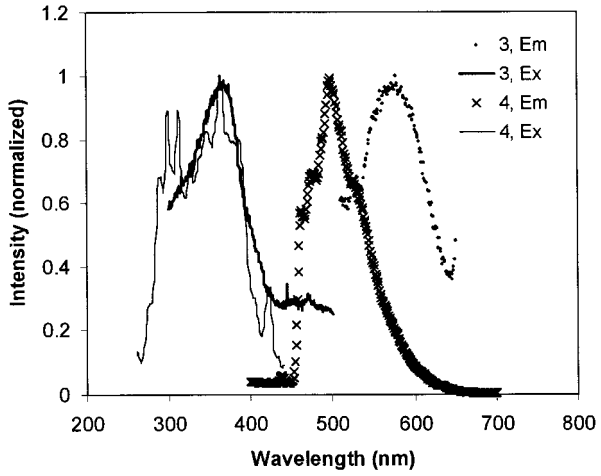

Figure 5. Excitation and emission spectra of **3** and **4** in the solid state at 77 K.

ture and display weak yellow-orange luminescence in the solid state. The orange luminescence of Pd(II) complexes **1**, **3**, and **5** is only detectable at 77 K in the solid state. In contrast, the Pt(II) complexes **2** and **4** have a visible yellow-orange luminescence at ambient temperature in the solid state. The emission maximum of **2** and **4** in the solid state shifts to the yellow-green region at 77 K. At 77 K in solution, only compound **2** yielded detectable yellow-green luminescence with a broad emission band ranging from 400 to 600 nm (λ_{max} = 464, 492 nm) and a long emission lifetime, 241 ± 3 μs, indicating the emission is phosphorescent. The emission spectra of **1**, **3**, and **5** in the solid state have a similar shape and are in the same energy region. For comparison purposes, the spectra of **3** and **4** at 77 K in the solid state are shown in Figure 5. The luminescent data of **1**−**5** along with those of the corresponding ligands are summarized in Table 3. Among all five compounds, in the solid state only compound **4** displays sufficiently bright emission that allows the measurement of emission lifetime. The emission lifetime of **4** in the solid state was determined to be 16 ± 2 μs at 298 K and 414 ± 1 μs at 77 K, indicating that the emission is likely phosphorescent. Since the crystal structures of **1**−**5** did not reveal any significant metal−metal interactions, contributions from metal−metal interactions to the emission can be ruled out. Two remaining possibilities for the cause of the emission are charge transfer between the metal and the chelate ligand or ligand-centered $\pi^* \rightarrow \pi$ transitions.[1] To understand the nature of luminescence displayed by **1**−**5**, we carried out molecular orbital calculations for compounds **1**−**4** by using extended Huckel methods.[11] The molecular geometry was established by using the crystallographic coordinates of compounds **1**−**4**. The LUMO orbitals for both compounds **1** and **2** are similar and characteristic π^* orbitals centered on the Bab ligand with little metal contributions (the LUMO of **1** is shown in Figure 6). The HOMO orbital for **1** consists of mostly the d(z^2) orbital of the Pd(II) ion and the σ orbitals of the ligand. In contrast, the HOMO of **2** is mostly π orbitals from the Bab ligand with substantial contributions from the d(yz) orbital of the Pt(II) center. On the basis of the results of EHMO calculations, the electronic transition in compound **1** could be considered as a charge-transfer transition between d(z^2) of the Pd(II) ion and the π^* orbital of the Bab ligand, while the electronic transition in compound **2** could be best described as a π (Pt and Bab) to π^* (Bab) transition. The LUMO levels for **3** and **4** are π^* orbitals, similar to those of **1** and **2**. The HOMO of **3** is a π orbital similar to that of **2** but with a significant contribution from the bromine atom. The second HOMO of **3** consisting of mostly the d(z^2) orbital of the Pd(II) ion and some σ orbitals of the ligand has an energy slightly lower than that of the HOMO and is similar to the HOMO of **1**. The participation of the bromine p_π lone pair orbital in the π orbital of the Pd ion and the Br−Bab ligand apparently raises the π energy level such that it is slightly above the energy level of the d(z^2) orbital of the Pd(II) ion. As a result, the electronic transition in **3** could be either a charge-transfer transition similar to that of **1** or a π to π^* transition similar to that of **2**. The LUMO and HOMO levels of compound **4** are similar to those of **2** except that a significant contribution from the bromine atom is present in the HOMO level. Therefore, the electronic transition in compound **4** is most likely a π to π^* transition similar to that of **2**. The calculated band gap

(11) Mealli, C.; Proserpio, D. M. *J. Chem. Educ.* **1990**, *67*, 399. (b) Ammeter, J. H.; Bürgi, H.-B.; Thibeault, J. L.; Hoffmann, R. *J. Am. Chem. Soc.* **1978**, *100*, 3686. (c) Hay, P. J.; Thibeault, J. C.; Hoffmann, R. *J. Am. Chem. Soc.* **1975**, *97*, 4884.

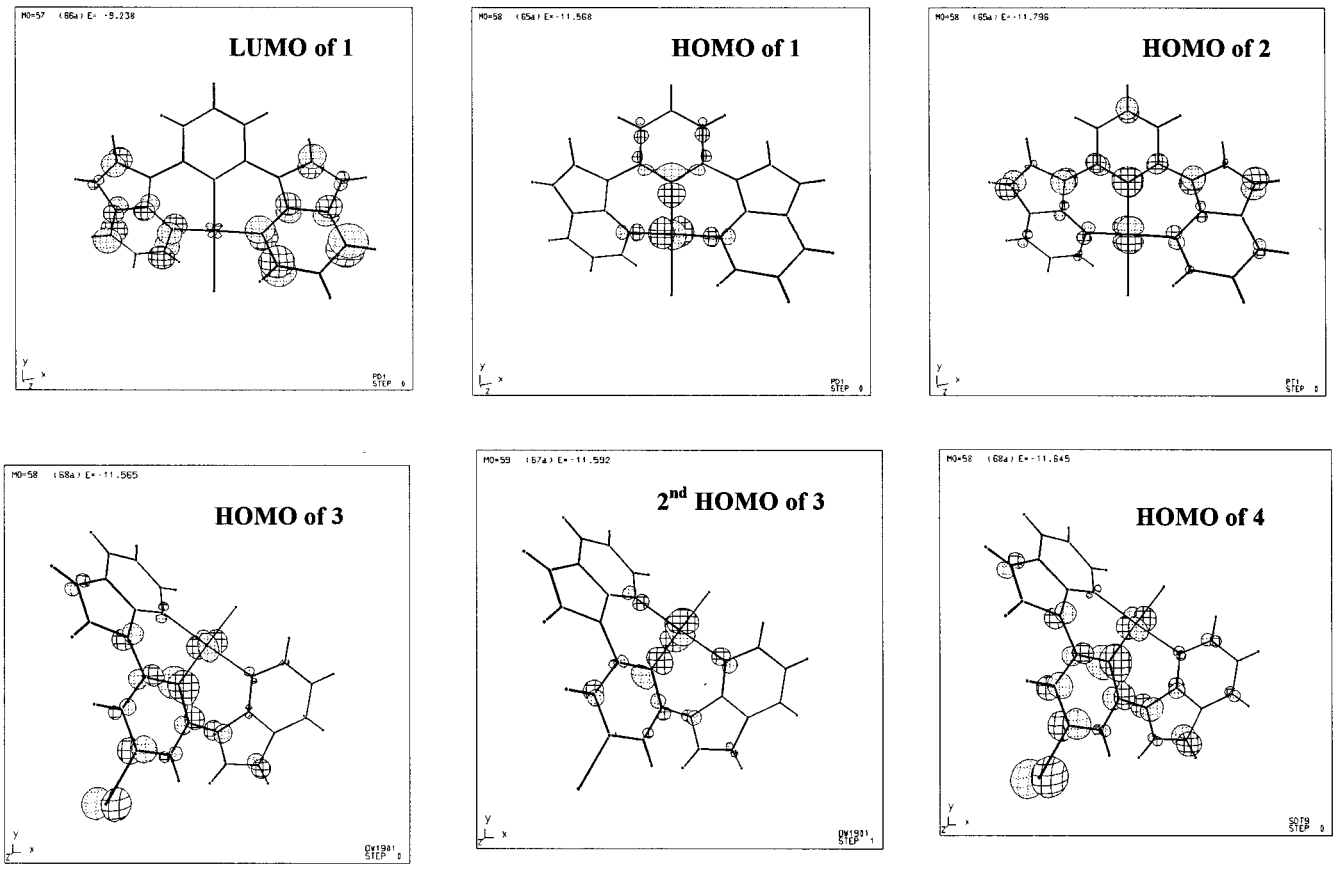

Figure 6. LUMO of **1** (LUMOs of **2**, **3**, and **4** have a similar appearance and therefore are not shown), HOMOs of **1** and **2**, HOMO and second HOMO of **3**, and HOMO of **4**.

of **4** is smaller than that of **2**, again attributable to the bromine p_π lone pair participation in the HOMO level of **4** and is consistent with the fact that the observed excitation energy of **2** is significantly higher than that of **4**. The free ligands BabH, Br−BabH, and TabH are bright blue emitters. The fact that orange/yellow-green luminescence was observed in their Pd(II) and Pt(II) complexes can be attributed to the removal of the ortho proton from the free ligand, which is known to decrease the energy gap and the participation of d lone pair electrons of the metal center in the HOMO level (in the Pt(II) complexes, the d lone pair participation in the π orbital further decreases the LUMO−HOMO energy gap.).

Current efforts by our group focus on the replacement of the chloride ligand in **1**−**5** by nitrogen and carbon σ donors and the systematic examination of the effect of the σ donors on luminescence of the Pd(II) and Pt(II) complexes, which could reveal additional information on the electronic properties of complexes **1**−**5**.

In summary, five new Pd(II) and Pt(II) complexes based on the 7-azaindolyl derivative ligands Bab, Br−Bab, and Tab have been synthesized. These new complexes display weak luminescence in the solid state, which is most likely caused by π to π^* transitions in the Pt(II) complexes and d(z^2) or π to π^* transitions in the Pd(II) complexes.

Acknowledgment. We thank the Natural Sciences and Engineering Research Council of Canada, Canada Foundation for Innovation, and the Xerox Research Foundation for financial support.

Supporting Information Available: Details of crystal structural analyses, tables of atomic coordinates, complete lists of bond lengths and angles, anisotropic thermal parameters and hydrogen parameters, diagrams showing the crystal structure of Br−BabH, the crystal lattice of TabH, the disordered portion of compound **1**, and the stacking of molecules of **2** and **4** in the crystal lattices. This material is available free of charge via the Internet at http://pubs.acs.org.

OM010235Z